ЖУРНАЛ СТРУКТУРНОЙ ХИМИИ

2011. Том 52, № 2 *Март – апрель* *С. 412 – 418*

UDC 541.6:547.24

STRUCTURAL AND PHOTOPHYSICAL CHARACTERIZATION, TOPOLOGICAL AND CONFORMATIONAL ANALYSIS OF 2-*o*-TOLYL-4-(3-N,N-DIMETHYLAMINOPHENYLMETHYLENE)-OXAZOL-5-ONE

© 2011 **R. Sevinçek[1]*, G. Öztürk[2], M. Aygün[1], S. Alp[2], O. Büyükgüngör[3]**

[1]*Department of Physics, Faculty of Arts & Sciences, Dokuz Eylül University, Buca, 35160-İzmir, Turkey*
[2]*Department of Chemistry, Faculty of Arts & Sciences, Dokuz Eylül University, Buca, 35160-İzmir, Turkey*
[3]*Department of Physics, Faculty of Arts & Sciences, Ondokuz Mayıs University, Kurupelit, 55139-Samsun, Turkey*

Received September, 5, 2010

A novel oxazole-5-one derivative 2-*o*-tolyl-4-(3-N,N-dimethylaminophenylmethylene)-oxazol-5-one (TDPO) $C_{19}H_{18}N_2O_2$ is synthesized and characterized and the crystal structure is determined by X-ray crystallography. TDPO is monoclinic in the $P2_1/c$ space group. The molecule adopts the Z configuration. To enlighten the flexibility of TDPO, the selected torsion angle is varied from –180° to 180° in each 10° separately, and the molecular energy profile is calculated and analyzed by density functional calculations. In addition, Bader′s QTAIM analysis is performed to investigate the intramolecular weak interactions.

K e y w o r d s: crystal structure, oxazole-5-one, conformational analysis, topological analysis.

INTRODUCTION

Oxazole-5-one (azlactone) derivatives are important as intermediates for the synthesis of several biologically active molecules. They are also precursors of amino acids containing an aromatic side chain. A number of methods are available for the synthesis of azlactones including the recent use of anhydrous zinc chloride or bismuth (III) acetate as a catalyst [1].

4-Benzylidene-2-phenyloxazole-5-one was first prepared at the beginning of the 20th century and has been the subject of much attention since then for various applications. The preparations of addition polymer sand polyamides from alkenyl azlactones and bisazlactones has been reported by Drtina et al. [2].

In spite of wide range applications of azlactones arising from the luminescence behavior and structural characteristics, there appear to be limited data on the luminescence properties. The fluorescence behavior of azlactone derivatives were investigated in the solid and liquid states and the studies have shown favourable photophysical and photochemical properties in the crystalline state, which has resulted in their use in semiconductor devices such as electrophotographic photoreceptors and in nonlinear optical materials [3].

Here, we report synthesis, structural and photophysical characterization, molecular and crystal structure, and topological analysis of TDPO.

EXPERIMENTAL

UV-Vis absorption spectra were recorded on a Shimadzu UV-1601 spectrophotometer. Fluorescence measurements were performed using a Varian-Cary Eclipse spectrofluorimeter. The ^{1}H NMR spectra were recorded on a Varian Mercury AS 400 NMR spectrometer at 400 MHz.

* E-mail: resul.sevincek@deu.edu.tr

Polymer Film, Polyvinyl Chloride (PVC) Preparation. A mixture for the membrane preparation was obtained by dissolving 120 mg of PVC, 240 mg of plasticizer, and a stochiometric amount of PTCPB with TDPO in 1.5 ml of dried THF. The concentration of DTPO in the mixture was about 2 mmol dye/kg polymer. The resulting cocktails were spread onto a 125 mm polyester support (Mylar TM type). The polymer support is optically fully transparent, ion impermeable and exhibits good adhesion to PVC. Sensor slides were kept in a dessicator, therefore the damage from the ambient air of laboratory was avoided.

Synthesis. A solution of N,N-dimethylaminobenzaldehyde (0.5 g; 3.5 mmol), 4-*o*-tolylglycine (0.6 g; 3.5 mmol), acetic anhydride (0.6 ml, 3.5 mmol), and sodium acetate (0.5 g; 3.5 mmol) was heated until the mixture just liquefied, and then heating was continued for further 2 h. After completion of the reaction (determined by thin-layer chromatography), ethanol (20 ml) was added and the mixture was kept at room temperature for 18 h. The solid product thus obtained was purified by washing with cold ethanol, hot water, and then a small amount of hexane. The solid was recrystallized from hot ethanol, and pure crystals were obtained.

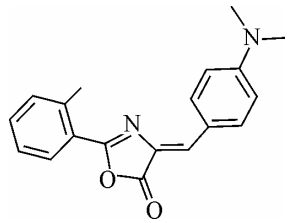

Scheme 1. Chemical diagram of TDPO

Spectroscopic Studies. ^{1}H NMR of 2-*o*-tolyl-4-(3-N,N-dimethylaminophenylmethylene)-oxazol-5-one ($CDCl_3$, 400 MHz, δ (ppm)): 2.83 (s, 3H, —C_6H_4—$\underline{CH_3}$); 3.09 (s, 6H, $(CH_3)_2N$—); 6.74—6.72, 8.10—8.08 (d, d 2H, 2H $(CH_3)_2N$—C—$\underline{CH}$=CH—, $(CH_3)_2N$—C—CH=$\underline{CH}$—); 7.26 (s, 1H, $(CH_3)_2N$—C_6H_4—$\underline{CH}$=); 7.34—7.33 (d, 1H, —$\underline{C_6H_4}$—CH_3); 7.43—7.39 (t, 2H, —$\underline{C_6H_4}$—CH_3); 8.06—8.04 (d, 1H, —$\underline{C_6H_4}$—CH_3).

Table 1 summarizes the excitation and emission related data: excitation and emission wavelengths, λ (nm), Stokes shift values, Δλ (nm), and singlet energy values, E_s (kcal/mol) of DTPO in solutions and plasticized PVC matrix. In all of the employed solvents and PVC matrix, the excitation wavelength was chosen as 450 nm and the emission spectra were recorded. In comparison to the solution phase, both absorption and emission maxima of TDPO in PVC matrix exhibited red shifts ranging from 6 to 27 nm (Table 1). These slight red shifts were presumably due to an increase in the polarity of the microenvironment of DTPO dye.

The TDPO dye exhibited moderate results concerning the Stokes shift values that range from 54 to 75 nm in all of the employed media. The highest Stokes shift was observed in PVC matrix, which indicates the advantage of better spectral resolution in emission-based studies and a desired property in commercially important dyes. The singlet energy of TDPO in the polymer film matrix E_s = 52.1 kcal/mol is observed to be slightly lower than that in the solvents. Apart from the larger Stokes shift, a higher radiative lifetime and lower singlet energy are also desirable fluorophore characteristics.

The photostability of the azlactone dye in PVC matrix was monitored and recorded on a steady-state spectrofluorimeter in the mode of time-based meas

Table 1

UV-vis absorption maxima, λ_{max}^{abs} (nm), *emission maxima*, λ_{max}^{emis} (nm), *Stokes shift*, Δλ (nm), *molar extinction coefficient*, ε ($L \cdot mol^{-1} \cdot cm^{-1}$), *and singlet energy*, E_s (kcal/mol) *of* 2-*o*-*tolyl*-4-(3-*N*,*N*-*dimethylaminophenylmethylene*)-*oxazol*-5-*one in DCM*, *ACN*, *and THF solvents and the polymer matrix* (*PVC*)

Solvent	λ_{max}^{abs}	λ_{max}^{emis}	Δλ	ε	E_s
DCM	467	521	54	217 000	54.9
ACN	464	538	74	209 000	53.0
THF	462	522	60	540 000	54.7
PVC	473	548	75	540 741	52.1

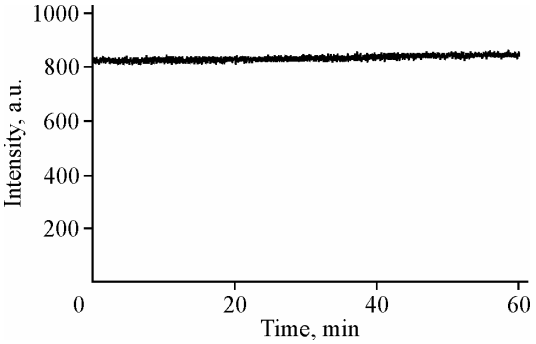

Fig. 1. Photostability test results of DTPO in PVC after 1 h of monitoring

urements. The data acquired at 548 nm correspond to the emission wavelength maximum of DTPO. The acquired data was obtained by using the excitation wavelength of 450 nm. The data collected after 1 h of monitoring shown in Fig. 1, reveals that PFO exhibits excellent photostability in PVC matrix.

X-ray Crystallographic Details. A suitable sample with the dimensions of 0.52×0.32×0.12 mm was selected for the crystallographic study. All diffraction measurements were performed at room temperature (296 K) using graphite monochromated MoK_α radiation of 0.71073 Å wavelength and a STOE IPDS II diffractometer. Accurate cell parameters and orientation matrix were determined by the least-squares refinement of the setting angles for 14228 reflections collected in the range $1.94 < \theta < 27.52°$. The systematic absences and intensity symmetries indicated the monoclinic $P2_1/c$ space group. Total 20714 reflections in the range $\theta_{min} = 1.94°$ and $\theta_{max} = 27.54°$ were collected in the rotation mode. The intensities were corrected for Lorentz and polarization factors, but not for the absorption effect ($\mu = 0.085 mm^{-1}$).

The structure was solved by direct methods using SHELXS-97 [4]. The structure was refined (on F^2) using full-matrix least-squares methods on the positional and anisotropic temperature parameters of the non-hydrogen atoms and isotropic temperature parameters for H atoms. The scattering factors were taken from SHELXL-97 [4]. The data collection conditions and parameters of the refinement process are listed in Table 2. CIF file containing complete information on TDPO was deposited with CCDC, deposition number 744697, and is freely available upon request from the following web site: www.ccdc.cam.ac.uk/data_request/cif.

T a b l e 2

Crystallographic data for TDPO

Color/shape	Red/prism
Chemical formula	$C_{19}H_{18}N_2O_2$
Formula weight	306.36
Temperature, K	296
Crystal system	Monoclinic
Space group	$P2_1/c$
Unit cell dimensions	
a, *b*, *c*, Å	6.5964(4), 11.4230(8), 21.6125(11)
β, deg.	104.159(4)
Volume, Å^3	1579.04(17)
Z	4
Density (calculated), g/cm^3	1.29
Absorption coefficient, mm^{-1}	0.085
Diffractometer/meas. meth.	STOE IPDS II/rotation
θ range for data calculation (deg.)	1.9—27.5
Unique reflections measured	3638
Independent/Observed ($I > 2\sigma(I)$) reflections	3638/2119
Data/restraints/parameters	3638/0/270
Goodness-of-fit on F^2	0.921
Final *R* indices [$I > 2\sigma(I)$]	$R_1 = 0.039$, $wR_2 = 0.084$
R indices (all data)	$R_1 = 0.081$, $wR_2 = 0.096$

Computational Details. The geometry optimization of the molecule leading to the energy minima was achieved by DFT calculations with the use of the B3LYP [5] hybrid exchange correlation functional with the 6-311G(*d*,*p*) [6] basis set. In order to determine the most stable conformation, the selected torsion angle T1 (N1—C10—C11—C12) is varied from –180° to 180° in 36 steps, and the molecular energy profile is obtained by performing single point energy calculations on the calculated potential energy surface. All calculations were performed using Gaussian 03W [7].

The Bader′s ″Quantum Theory of Atoms in Molecules″ (QTAIM) was also applied [8, 9]. The analysis of electron density distributions was performed to find the bond critical points [10, 11] and to characterize them in terms of electron densities and their Laplacians. The QTAIM calculations were carried out using the AIM2000 program [12].

RESULTS AND DISCUSSION

Crystallographic Analysis. An ORTEPIII diagram [13] with the atom numbering scheme and the packing diagram in the unit cell are shown in Figs. 2 and 3 respectively. Comparative results obtained from X-ray crystallography and computational studies are listed in Table 3.

The bond distances and the bond angles of the oxazolone ring such as N1—C8, N1—C10, C10—C11 bond distances, C8—C10—C11, N1—C10—C9, N1—C10—C11 bond angles can be compared with those in similar compounds [14—18]. The oxazolone ring makes dihedral angles of 4.06(11)° and 0.60(11)° with PL1 (C1…C6 plane) and PL2 (C12…C17 plane) respectively. The maximum deviations from the mean oxazolone ring plane are 0.003(1) and –0.003(1) Å for C8 and O1 respectively. There is a C—H…N type intramolecular interaction (with the C17—H17 parameters of 0.97 Å, H17…N1 of 2.37 Å, C17…N1 of 3.044 Å, ∠C17—H17…N1 of 127°), as shown in Fig. 2.

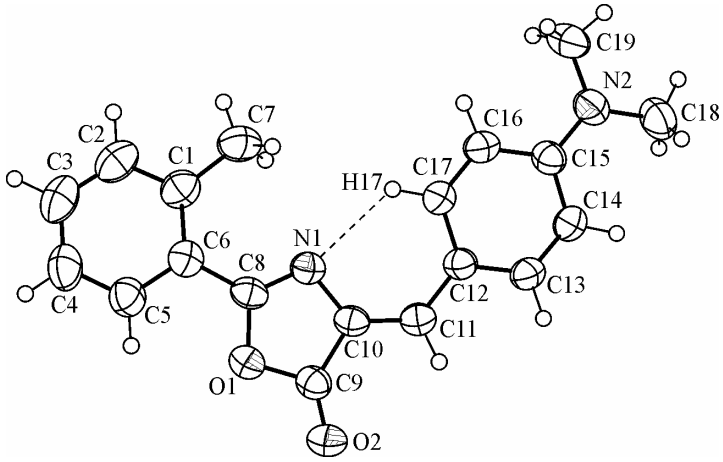

Fig. 2. An ORTEP III view of TDPO with atomic numbering of non-H atoms. Displacement ellipsoids are shown at the 50 % probability level. Dashed line presents the C—H···N type intramolecular weak interaction

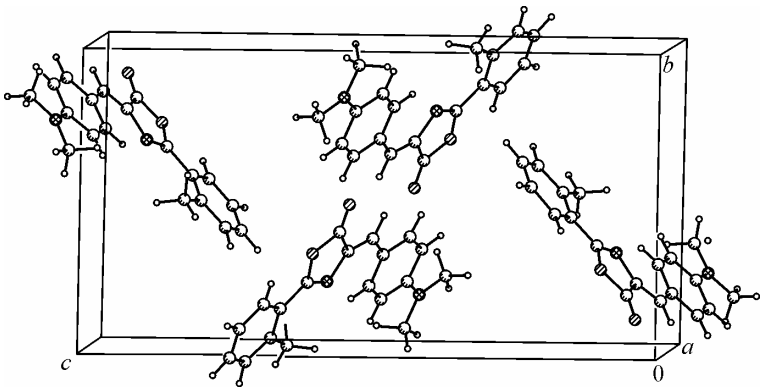

Fig. 3. Packing diagram for TDPO

Table 3

Selected bond distances (Å), *bond and torsion angles* (deg.)

Bond distances	X-ray	B3LYP	Bond Angles	X-ray	B3LYP
O(1)—C(8)	1.388(2)	1.379	C(8)—O(1)—C(9)	105.8(1)	106.3
O(1)—C(9)	1.406(2)	1.408	C(8)—N(1)—C(10)	106.5(1)	106.1
O(2)—C(9)	1.198(2)	1.197	C(1)—C(6)—C(8)	122.2(1)	122.7
N(1)—C(8)	1.284(2)	1.294	N(1)—C(8)—O(1)	114.7(1)	115.0
N(1)—C(10)	1.397(2)	1.395	O(2)—C(9)—C(10)	134.6(1)	134.0
C(6)—C(8)	1.456(2)	1.461	N(1)—C(10)—C(9)	108.5(1)	108.6
C(10)—C(11)	1.357(2)	1.361	N(1)—C(10)—C(11)	127.7(1)	129.1
C(11)—C(12)	1.435(2)	1.438			
Torsion angles	X-ray	B3LYP	Torsion angles	X-ray	B3LYP
C(8)O(1)C(9)O(2)	–178.1(1)	179.9	N(1)C(10)C(11)C(12)	0.0(3)	0.0
C(1)C(6)C(8)N(1)	3.2(2)	–0.147	C(10)C(11)C(12)C(13)	176.1(2)	179.9

TDPO adopts the Z configuration at the C10=C11 olefinic bond. Since the conjugation of the π-electron system in the dimethylaminophenyl aromatic ring is reflected in the C—C bond lengths between the oxazolone and dimethylaminophenyl rings, the C10=C11 olefinic bond is slightly longer than the formal C=C double bond; and the C11—C12 single bond is slightly shorter than the formal C—C single bond.

Conformational Analysis. In order to obtain the most stable conformation of TDPO, the torsion angle t (N1—C10—C11—C12) was chosen since it determines the isomerism (E or Z). According to the crystallographic study, t is obtained as 0.0(3)°, whereas this torsion angle is –0.025° in the optimized molecular structure. DFT methods cannot comprehensively represent the structural properties of the crystalline materials because they have some foibles regarding as a single molecule (gas phase instead of the crystalline state) throughout the computations. For these reasons, some discrepancies are observed between the molecular conformations of the optimized and X-ray structures (Fig. 4).

The DFT molecular orbital calculations were carried out in order to define the conformational flexibility of TDPO as a function of the torsion angle t. Variation of the relative energy against the torsion angle t is shown in Fig. 5. The energy profile has a minimum in the vicinity of 0° (Z configuration). When the molecule is close to the E configuration , there are two local minima in the vicinity of –150° and 150°; there appears the C—H…O type intramolecular H-bond between H13 and O2

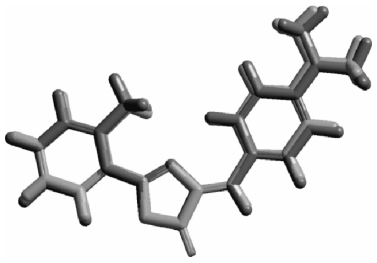

Fig. 4. Superposition of X-ray and optimized structures of TDPO. Red denotes X-ray results; blue denotes optimized geometry. RMSD value is $1.279 \cdot 10^{-2}$ Å

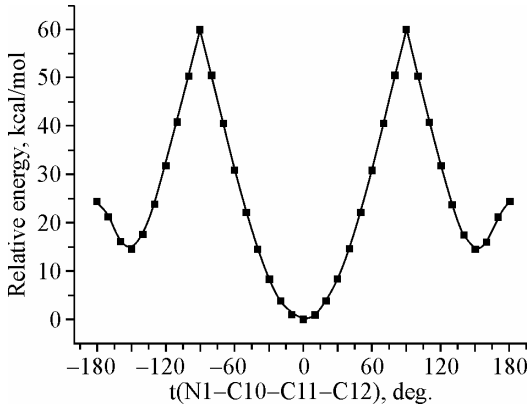

Fig. 5. Variation of the relative energy to the optimized structure versus selected torsion angle

Table 4

Selected topological parameters of TDPO (*all values are given in atomic units*)

	λ_1	λ_2	λ_3	ρ_c	$L[\rho_c]$	ε
C17—H17	–0.78313	–0.77353	0.54945	0.28705	0.25180	0.01241
N1…H17	–0.01242	–0.01173	0.06957	0.01317	–0.01136	0.05882
N1=C8	–0.89694	–0.70562	0.46302	0.37971	0.28488	0.27114
N1—C10	–0.63057	–0.57636	0.33361	0.30494	0.21833	0.09406
C10=C11	–0.70262	–0.54967	0.30384	0.32676	0.23711	0.27826
C11—C12	–0.57866	–0.51150	0.34084	0.28409	0.18733	0.13130

(d[O…H] = 1.923 Å at t = 150° and d[O…H] = 1.914 Å at t = –150°). According to the conformational analysis, there are two possible configurations: Z ($t \approx 0°$) or E ($t \approx \pm 150°$). The Z configuration is more stable than E, which is confirmed by the X-ray crystallographic results.

Topological Analysis. In QTAIM, bonds are described by bond critical points (BCPs) in terms of some topological parameters. such as the electron density at the critical point ρ_c and the corresponding Laplacian field $L[\rho_c] = -1/4\nabla^2\rho_c$ [19]. $\nabla^2\rho_c$ is defined as the sum of the eigenvalues of the diagonalized Hessian matrix of the electron density ($\nabla^2\rho_c = \lambda_1 + \lambda_2 + \lambda_3$). The ρ_c value is used to describe the bond strength; the larger ρ_c value corresponds to the stronger bond. The Laplacian field describes the characteristics of the bond; $L[\rho_c] > 0$ refers to the covalent bonding, $L[\rho_c] < 0$ intends to a closed-shell interaction (ionic bonding, hydrogen bonding or van der Waals interactions). Some topological parameters of TDPO are listed in Table 4.

Small values of two negative eigenvalues (λ_1 and λ_2) of the Hessian of BCP between H17 and N1 point out the low electron concentration at this BCP. The low value of the electron density ρ_c at BCP between N1 and H17 represents the weakness of this interaction. Also the negative sign of $L[\rho_c]$ indicates a closed-shell interaction.

Ellipticity ($\varepsilon = \lambda_1/\lambda_2 - 1$, $\lambda_1 > \lambda_2$) is a criteria of bond geometries. Some remarkable ellipticity values are: 0.0 for the single bond in ethane and the triple bond in acetylene; 0.23 for the CC bond in aromatic benzene; 0.45 for the formal double bond in ethylene [20]. Considering the results in Table 5, it can be stated that N1—C10 is a single bond, N1=C8 and C10=C11 are close to an aromatic bond character, and C11—C12 bond has distorted cylindrically symmetric geometry.

CONCLUSIONS

The TDPO dye exhibited moderate results concerning high Stokes shift values and excellent photostability in PVC matrix, which is a desired property in emission-based studies of commercially important dyes.

The molecular and crystal structure of TDPO has been determined by X-ray crystallography. In addition, conformational and topological analyses were performed. According to the results obtained by X-ray crystallography and the conformational analysis, TDPO is in the Z configuration corresponding to the minimum energy. It is also possible to say that the intramolecular H-bond plays an effective role in the molecular conformation profile. The intramolecular H-bond is also supported by the topological studies.

Acknowledgements. The authors would like to thank the Ondokuz Mayıs University Art and Sciences Faculty for the use of the STOE IPDS II Diffractometer purchased under grant No. F279, and the Dokuz Eylül University Research Fund (project number: 2007.KB.FEN.36 and 04.KB.FEN.024) for the support of this work. In addition, RS thanks TÜBİTAK (The Scientific and Technical Research Council of Turkey) for partial support.

REFERENCES

1. *Paul S., Nanda P., Rajive G. et al.* // Tetrahedron Lett. – 2003. – **45**, N 2. – P. 425 – 427.
2. *Drtina G., Haddad G., Rasmussen J. et al.* // React. Funct. Polym. – 2005. – **64**, N 5. – P. 13 – 24.
3. *Ertekin K., Alp S., Karapire C. et al*. // J. Photochem. and Photobio. A. – 2000. – **137**, N 2-3. – P. 155 – 161.
4. *Sheldrich G.M.* SHELX-97, release 97-2. – Germany, University of Goettingen, 1998.
5. *Hertwig R.H., Koch W.* // Chem. Phys. Lett. – 1997. – **268**, N 5-6. – P. 345 – 351.
6. *Hehre W.J., Ditchfield R., Pople J.A.* // J. Chem. Phys. – 1972. – **56**, N 5. – P. 2257 – 2261.
7. *Frisch M.J., Trucks G.W., Schlegel H.B. et al*. Gaussian 03, Revision B.05 – Gaussian Inc., Pittsburgh PA, 2003.
8. *Bader R.F.W.* // Acc. Chem. Res. – 1985. – **18**, N 1. – P. 9 – 15.
9. *Bader R.F.W.* // Chem. Rev. – 1991. – **91**, N 5. – P. 893 – 928.
10. *Carrol M.T., Chang C., Bader R.F.W.* // Mol. Phys. – 1988. – **63**, N 3. – P. 387 – 405.
11. *Carrol M.T., Bader R.F.W.* // Mol. Phys. – 1988. – **65**, N 3. – P. 695 – 722.
12. *Biegler-König J., Schönbohm D. Bayles D.* // J. Comput. Chem. – 2001. – **22**, N 5. – P. 545 – 559.
13. *Farrugia L.J.* // J. Appl. Cryst. – 1997. – **30**, N 5-1. – P. 565.
14. *Şen B., Öztürk G., Alp S. et al*. // Acta Crystallogr. – 2007. – **C63**, N 4. – P. o223 – o224.
15. *Sun Y.-F., Wang X.-L., Li J.-K. et al*. // Acta Crystallogr. – 2007. – **E63**, N 11. – P. o4426.
16. *Sun Y.-F., Cui Y.-P.* // Acta Crystallogr. – 2008. – **E64**, N 4. – P. o678.
17. *Asiri A.M., Akkurt M., Khan I.U. et al*. // Acta Crystallogr. – 2009. – **E65**, N 4. – P. o842.
18. *Sevinçek R., Öztürk G., Aygün M. et al*. // Spect. Lett. – 2009. – **42**, N 1. – P. 1 – 6.
19. *Bader R.F.W.* Oxford University Press Inc., New York, 1990.
20. *Matta C.F., Boyd R.J.* WILEY-WCH, Verlag GmbH & Co. KGaA, Weinheim, 2007.